

1 Original Article

2 **Distribution of seasonal variation of point refractivity gradient and geo-climatic**  
3 **factor over Ede-Nigeria**

4 Sanyaolu Modupe

5 Department of Physical Sciences, Faculty of Natural Sciences, Redeemer's University,

6 Ede, 232103, Nigeria

7 \* Corresponding author, Email address: [sanyaolum@run.edu.ng](mailto:sanyaolum@run.edu.ng)

8  
9 **Abstract**

10 The quantification of anomalies in radio signal transmission has been a serious  
11 challenge using data from radiosondes to determine meteorological parameters in Ede,  
12 Nigeria. The point refractivity gradient and geoclimatic factor were analysed in this  
13 paper. Air temperature, relative humidity, and pressure for five years (2017 – 2021) are  
14 the meteorological parameters used. These parameters were collected from the ERA5  
15 (European Centre for Medium-Range Weather Forecasts, 2017) radiosonde data  
16 archives. The results revealed the monthly and seasonal fluctuations in the point  
17 refractivity gradient and geoclimatic component within the study period. From the  
18 results, Geoclimatic Factor (K) and the yearly average Point Refractivity Gradient ( $dN_1$ )  
19 for Ede are  $3.37E-05$  and  $-143.712$  N-units/Km respectively. In July, the highest  $dN_1$   
20 value of  $-48.332$  N-units/Km was recorded, while the lowest value of  $-225.534$  N-  
21 units/Km was recorded in November. In addition, the wet season has a higher point  
22 refractivity gradient than the dry season, although the wet season has a lower  
23 geoclimatic factor. The values obtained in this study are to be considered and adopted  
24 for better microwave link Quality of service (QoS) and availability in this region.

25

26 **Keywords:** Temperature, relative humidity, seasons, geoclimatic factor, Point  
27 refractivity gradient.

28

## 29 **1. Introduction**

30 The complexity of the troposphere is increased by atmospheric meteorological  
31 characteristics, such as water vapor density, temperature, relative humidity, and  
32 pressure, which have a substantial impact on microwave transmission. They interact in a  
33 variety of ways in the tropics to influence the propagation of radio waves, as well as the  
34 radio refractivity gradient (Zheng & Han-Xian, 2013; Zubair, Haider, Khan, & Nasir,  
35 2011). Behaviour of radio signals in the atmosphere is determined by establishing the  
36 variations of the refractivity gradient The vertical profiles of moisture, pressure, and air  
37 temperature in the atmosphere are responsible for this fluctuation (Emmanuel, Ojo, &  
38 Adedayo, 2020). When it comes to the transmission of radio waves during clear air on  
39 terrestrial line-of-sight lines, different behaviour of these atmospheric characteristics  
40 results in signal losses on the transmission link (Mason, 2010; Shambayati, 2008). The  
41 effects of super-refraction and ducting phenomena on radar observations and the  
42 refractivity gradient in a 1 km region above ground are significant for estimating super-  
43 refraction and ducting phenomena. The field strength at very high frequency (VHF)  
44 sites beyond the horizon also, cannot be underestimated (Bean & Dutton, 1968; Dairo &  
45 Kolawole, 2017; Karagianni, Mitropoulos, Latif, Kavousanos-Kavousanakis, Koukos,  
46 & Fafalios, 2014).

47 The subject of radio refractivity has received more attention, especially in the  
48 temperate region regarding this subject matter. Among such studies are the works of;  
49 Abdulhadi, & Kifah, 2010; Řezáčová, Ondřej, & Lucas, 2003; Valma, Tamosiunaite,

50 Tamosiunas, Tamosiuniene, & Zilinskas, 2011 to mention but a few. The attention is  
51 much needed in the tropics such as Ede in Nigeria due to the nature of its **intense**  
52 climatological environment.

53 In Nigeria, the likes of (Ojo, Ajewole, Adediji, & Ojo, 2015; Adediji &  
54 Ajewole, 2008; Adeyemi & Emmanuel, 2011; Asiyo & Thomas, 2013; Ele & Nkang,  
55 2014; Kolawole, 1983; Falodun & Ajewole, 2006; Ononiwu & Constance, 2015) had  
56 earlier worked on refractivity gradients and point refractivity gradients. However, one  
57 of the elements employed in determining multipath fade depth on communication **links**  
58 at any location of interest is the geoclimatic component. The utilization of  
59 meteorological characteristics collected in the lower and upper atmosphere is used to  
60 determine geoclimatic factors primarily.

61 Multipath fading arises when a signal encounters an obstruction that causes it to  
62 take multiple pathways before reaching its destination. As a result of this issue, signal  
63 propagation in the troposphere is hampered. Multipath fading can also be caused by **the**  
64 differing refractive index of the atmospheric horizontal layers in **particular**. This is in  
65 agreement with Serdege and Ivanovs (2007), **who** affirmed that due to seasonal  
66 variations in refractive index, radio wave systems may become unavailable and that the  
67 structure of the radio refractive index,  $n$ , in the lower atmosphere is a significant factor  
68 in communication connection estimation.

69 In addition, the notion of geoclimatic factor assessment is still important to  
70 communication engineers, because it stands as the most essential **criterion** in  
71 determining fade depth. The geoclimatic factor is used to calculate the likelihood of a  
72 worst-case month outage (Bettouche, Basile, & Kouki, 2014; Göktas, 2015; Ugwu,  
73 2015). The point refractivity gradient ( $dN_1$ ), which is determined by **several**

74 meteorological variables like temperature, pressure, and atmospheric vapour pressure, is  
75 used to calculate geoclimatic factors. The data is necessary for making adequate **plans**  
76 **and designs** for communication radio links for satellite networks, radar, and other  
77 applications.

78 The climate in Ede, Nigeria is hot and humid most of the year and is likely to  
79 experience anomalous propagation due to its special climate. In this regard, few studies  
80 are available for this region.

81 This study aims at estimating the seasonal variations in the geoclimatic factor values  
82 and point refractivity **gradient in Ede**, Nigeria.

83

84

## 85 **2. Materials and Methods**

86 Ede (Geo. 7.299° N, 5.147° E) in Nigeria's Osun state was chosen as the research  
87 area. The meteorological data used in this study was gathered over a five-year period  
88 (January 2017 to December 2021) from the archives of European Centre for Medium-  
89 Range Weather Forecasts, 2017 (ECMWF) Fifth generation atmospheric re-analysis  
90 (ERA-5) which provides hourly meteorological data (relative humidity, pressure, and  
91 temperature) required for characterisation of propagation conditions. ERA-5 uses  
92 complex modeling and data assimilation technologies to turn massive volumes of  
93 historical data into global estimations. It gives an hourly worldwide value of  
94 atmospheric parameters with 137 vertical levels from the surface to 0.01 hPa and a  
95 horizontal resolution of 31 km (Hersbach, 2016). Variations of wind regimes and near-  
96 surface air temperature are presented by ERA5. The ERA5 data being in NetCDF

97 format is downloaded and processed using the ferret and python packages (Tetzner,  
98 Thomas & Allen, 2019).

99 In Ede, the wet season usually **ranges** between the later end of March to  
100 September **end**, and the dry season most times pick up from October till February.  
101 Values of temperature, relative humidity, and pressure were gathered for five years from  
102 the daily log of Era5. These data were used to calculate the point refractivity gradients.  
103 The refractive index,  $n$ , can be represented by the term ‘radio refractivity,  $N$ ’ as defined  
104 by the International Telecommunication Union (ITU-R) (2012).

$$105 \quad N = (n - 1) \times 10^6 \quad (1)$$

$$106 \quad n = 1 + N \times 10^{-6} \quad (2)$$

107 In terms of measurable meteorological parameters, the refractivity  $N$ , can be expressed  
108 as :

$$109 \quad N = \frac{77.6}{T} \left( P + 4810 \frac{e}{T} \right) = 77.6 + \frac{P}{T} + 3.73 \times 10^5 \frac{e}{T^2} \quad (3)$$

110 where  $p$  denotes atmospheric pressure in hPa,  $T$  denotes absolute temperature in degrees  
111 Celsius (K), and  $e$  denotes water vapour pressure in hPa.

112 The dry and wet compositions of refractivity in the lower atmosphere (troposphere) are  
113 distinguished. The dry term makes up a larger portion of the total refractivity in the  
114 atmosphere, accounting for roughly 70% of the total value. The dry term varies with the  
115 distribution of gas molecules in the atmosphere and is proportional to their density.  
116 Surface data of pressure,  $P$  (hpa), and temperature,  $T$  (Kelvin) can be used to estimate  
117 the dry term of refractivity, which is reasonably stable, with an accuracy of about 20%.

$$118 \quad N_{\text{dry}} = 77.6 + \frac{P}{T} \quad (4)$$

119 The wet term, on the other hand, is responsible for the majority of the change in  
120 refractivity in the atmosphere. Due to the polar structure of water molecules, the term  
121 "wet" is used.

$$122 \quad N_{\text{wet}} = 3.73 \times 10^5 \frac{e}{T^2} \quad (5)$$

123 e, the water vapour pressure, is calculated by

$$124 \quad e = \frac{6.112H}{100} \exp\left(\frac{17.502t}{t+240.97}\right) \quad (6)$$

125 H (%) denotes relative humidity, and t (°C) denotes air temperature.

126 The refractivity gradient in the atmosphere which is a function of height is expressed as  
127 (ITU, 2003):

$$128 \quad \frac{dN}{dh} \approx \frac{N_2 - N_1}{h_2 - h_1} \quad (7)$$

129 where  $N_1$  and  $N_2$  are the refractivity at heights  $h_1$  and  $h_2$  respectively.

130  $N_1$  and  $N_2$  are the lower and upper atmospheric refractive indexes, respectively.

131 (Chaudhary & colleagues, 1986).

132 The point refractivity  $dN_1$  (N – units/Km) according to ITU-R P.530-15 (09/2013) is the  
133 point refractivity gradient in the lowest 65 m of the atmosphere not exceeded for 1% of  
134 an average year. The  $dN_1$  value is obtained using (7), where  $N_1$  is calculated considering  
135 the  $h_1$  value nearest to 65 m height, so that  $60 \text{ m} < h_1 < 70 \text{ m}$

136 Inverse Distance Weighting (IDW) is a method of spatial interpolation that is employed  
137 in data analysis when a collection of missing points or no observations are available.

$$138 \quad Z_0(x_0) = \sum_i^n \lambda_i (x_i) \quad (8)$$

139  $i$  represented the value approximated with respect to the observed points,  $x_0$ ,  $n$   
140 **represents** the total number of points that were sampled.  $Z$ , **represents** the known value  
141 at the sampled point,  $\lambda_i$  and  $x_i$  are the weighting parameters.

142 
$$\frac{\frac{1}{(d_i)^p}}{\sum_{i=1}^n \frac{1}{(d_i)^p}} \quad (9)$$

143  $d_i$  denotes the distance between  $x_o$  and  $x_i$ ,  $n$  is as mentioned earlier, and  $p$  is the power  
 144 factor.

145 The Geoclimatic factor  $K$  was calculated using ITU-R. P.530-14, 2012

146 
$$K = 10^{-4.6 - 0.0027d N_1} \quad (10)$$

147

148

### 149 **3. Results and Discussion**

150 The data in this study encompassed the two climatic seasons that occur in Ede  
 151 each year, the wet season and the dry season. Every year, the dry season is from  
 152 October to February, and the rainy season extends from March to September.

153 The Ede climate is tropical in nature; it is a zone where warm, wet air from the  
 154 Atlantic meets hot, dry, and often dusty air from the Sahara, known as the 'harmattan.'  
 155 Equation (6) was used to convert relative humidity to water vapour pressure,  $e$  (hpa),  
 156 while Equation (3) was used to calculate the refractivity using the data.

157 Figure 1 shows the yearly point refractivity gradient variations. The results **show**  
 158 that **the** year 2017 has the highest point refractivity gradient while the year 2020  
 159 recorded the lowest point refractivity. The average point refractivity gradient for the  
 160 five (5) years is estimated to be -158.39. This is attributed to the climatic changes  
 161 **during** that period. Ede experienced very low precipitation in the year 2020.

162 Table 1 and Figure 2 **show** the results obtained from the computed values of the  
 163 point refractivity gradient for the average monthly records. From March to August, high  
 164 levels of point refractivity were recorded, owing to the presence of high humidity

165 beginning in the month of March, as a result, there is a lot of water vapour pressure in  
166 the atmosphere, and could be attributable to the convective and occasionally  
167 thunderstorm forms of rain that were seen during this time. Due to heavy rainfall in the  
168 months preceding the event, the atmosphere experiences a lifting of the boundary layer,  
169 with significant amounts of water vapour present in the atmosphere (Adeyemi, 2004).  
170 The values of point refractivity were also seen to be low during the dry season. Figure 2  
171 depicts the usual monthly change of point refractivity at the start of the dry season in  
172 October, revealing an erratic oscillation. The measured point refractivity gradient values  
173 are projected to diminish by December as the harmattan haze begins to take impact and  
174 becomes intense. These findings are in agreement with the works of (Abdulhadi, &  
175 Kifah, 2010; Bettouche et al., 2014; Ilesanmi & Moses, 2021; Odedina & Afullo, 2007;  
176 Ojo, Ajewole, Adediji, & Ojo, 2015; Valma et al, 2011.

177 The point refractivity gradients' values at Ede vary greatly; the highest value of -  
178 48.33 N-units/Km was recorded in July, while the lowest value of -320.144 N-units/Km  
179 was recorded in November. The results also agree to an extent with the global ITU map  
180 which theoretically gives the threshold of  $dN_1$  in these coordinates to be -273.2 N/km.  
181 However, the variations in the values call for attention for the optimum performance of  
182 digital terrestrial point to point links in Ede.

183 In Table 1, it is seen that the Geoclimatic Factor (K) and annual average Point  
184 Refractivity Gradient ( $dN_1$ ) are  $3.37E-05$  and -143.712 N-units/Km respectively. Table  
185 2, and as reflected in Figure 3 and Figure 4, demonstrated seasonal fluctuations in the  
186 duo. -116.17 (N-units / Km) was recorded for the average point refractivity during the  
187 wet season while -182.271 (N-units / Km) was estimated for the average  $dN_1$  during the

188 dry season. Obviously, the point refractivity gradient ( $dN_1$ ) was higher in the wet season  
189 compared to the dry season.

190 The estimated values of the average Geoclimatic factor (K) were shown in Table  
191 3, and in Figure 4, for the wet season,  $3.1617E-05$  was estimated while  $3.68E-05$  was  
192 estimated for the dry season. As a result, the Geoclimatic factor in the dry season was  
193 higher compared to the wet season. In the dry season, the monthly range between March  
194 and September (rainy months), has lower values, whereas the dry season, which runs  
195 from October to November, has higher values. The results are in agreement with the  
196 works of Odedina & Afullo, 2007; Ilesanmi & Moses, 2021.

197

#### 198 **4. Conclusions**

199 Meteorological parameters, such as humidity, temperature, and air pressure, over  
200 Ede, Nigeria, are used to determine the geoclimatic factor and the point refractivity  
201 gradient in order to know the behaviour of radio waves in the area. This will give **the**  
202 **opportunity** to make appropriate decisions **regarding** the type of device, transmitter gain,  
203 public guide, and mitigation strategies to be employed in ensuring a smooth  
204 transmission of the radio waves in Ede. Monthly and seasonal fluctuations in the  
205 geoclimatic factor and point refractivity gradient were observed. The wet season has a  
206 higher point refractivity gradient than the dry season, but with a lower geoclimatic  
207 factor.

208

209

210

#### 211 **Acknowledgments**

212 I sincerely appreciate the effort of Copernicus Climate Change Service in  
213 making the Era5 data available for the purpose of research.

214

## 215 **References**

216 Abdulhadi, A., & Kifah, A. (2010). Calculation of Effective Earth Radius and Point  
217 Refractivity Gradient in UAE, Hindawi Publishing Corporation International  
218 *Journal of Antennas and Propagation*. 2010, Article ID 245070, 4 pages  
219 doi:10.1155/2010/245070

220 Adediji, A. T., & Ajewole, M. O. (2008). Vertical profile of radio refractivity  
221 gradient in Akure South-West Nigeria. *Progress in Electromagnetics Research*  
222 *C*, 4, 157–168. doi:10.2528/PIERC08082104

223 Adeyemi, B., & Aro, T. O., (2004). Variation in surface water vapour density over  
224 four Nigerian stations. *Nigeria Journal of Pure and Applied Physics*, 3(1), 38-  
225 44. doi:10.4314/njpap.v3i1.21454

226 Adeyemi, B., & Emmanuel, I. (2011). Monitoring tropospheric radio refractivity over  
227 Nigeria using CM-SAF data derived from NOAA-15, 16 and 18 satellites.  
228 *Indian Journal of Radio and Space Physics*, 40(6), 301-310,

229 Retrieved from

230 [https://www.academia.edu/11837471/Monitoring\\_tropospheric\\_radio\\_refractivit](https://www.academia.edu/11837471/Monitoring_tropospheric_radio_refractivit_y_over_Nigeria_Using_CM_SAF_data_derived_from_NOAA_15_16_and_18_Satellites)  
231 [y\\_over\\_Nigeria\\_Using\\_CM\\_SAF\\_data\\_derived\\_from\\_NOAA\\_15\\_16\\_and\\_18](https://www.academia.edu/11837471/Monitoring_tropospheric_radio_refractivit_y_over_Nigeria_Using_CM_SAF_data_derived_from_NOAA_15_16_and_18_Satellites)  
232 [Satellites](https://www.academia.edu/11837471/Monitoring_tropospheric_radio_refractivit_y_over_Nigeria_Using_CM_SAF_data_derived_from_NOAA_15_16_and_18_Satellites)

233 Asiyo, M. O., & Afullo, T. J. O. (2013). Statistical estimation of fade depth and  
234 outage probability due to multipath propagation in Southern Africa. *Progress in*  
235 *Electromagnetics Research B*, 46, 251-274. doi:10.2528/PIERB12101212

236 Bean, B. R., Dutton, E. J., & Central Radio Propagation Laboratory (U.S.). (1968).

237 *Radio Meteorology*. New York, NY: Dover Publication.

238 <https://nvlpubs.nist.gov/nistpubs/Legacy/MONO/nbsmonograph92.pdf>

239 Bettouche, Y., Basile, L. A., & Kouki B. A., (2014). Geoclimatic factor and point  
240 refractivity evaluation in Quebec-Canada. *XXXIth URSI General Assembly and*  
241 *Scientific Symposium (URSI GASS)*, 1-4.  
242 doi:10.1109/URSIGASS.2014.6929621

243 Chaudhary, N. K., Trivedi, D. K., & Roopam, G. (1986). Radio link reliability in  
244 Indian semi-desert terrain under foggy conditions. *International Journal of*  
245 *Latest Trends in Computing*, 2(1), 2-218.

246 Dairo, O. F., & Kolawole, L. B. (2017). Statistical analysis of radio refractivity gradient  
247 of the rainy-harmattan transition phase of the lowest 100 m over Lagos, Nigeria,  
248 *Journal of Atmospheric and Solar-Terrestrial Physics*, 167, 169-176.  
249 doi:10.1016/j.jastp.2017.12.001

250 European Centre for Medium-Range Weather Forecasts. ECMWF, Annual Report  
251 2017. <https://www.ecmwf.int/en/elibrary/18309-annual-report-2017>

252 Ele, I. E., & Nkang, M. O. (2014). Analysis of production determinants and technical  
253 efficiency in crayfish production in the lower cross river basin, Nigeria. *Quest*  
254 *Journals Journal of Research in Humanities and Social Science*, 2(11), 30-36.

255 Emmanuel, O. S., Ojo, A. O., & Adedayo. K. D. (2020). Geo-statistical distribution of  
256 vertical refractivity gradient over Nigeria. *Radio Science*, 55(9),  
257 doi:10.1029/2020RS007109

258 Falodun, S. E., & Ajewole, M. O. (2006). Radio refractive index in the lowest 100 m  
259 layer of the troposphere in Akure, South Western Nigeria. *Journal of*  
260 *Atmospheric and Solar-Terrestrial Physics*, 68(2), 236-243.  
261 doi:10.1016/j.jastp.2005.10.002

262 Göktas, P. (2015). Analysis and implementation of prediction models for the design of  
263 fixed terrestrial point-to-point systems. *Diss. bilkent university.*  
264 <http://www.thesis.bilkent.edu.tr/0006774.pdf>

265 Hersbach, H. (2016). The ERA5 Atmospheric Reanalysis. *American Geophysical*  
266 *Union*, Fall Meeting 2016, abstract #NG33D-01.  
267 <https://ui.adsabs.harvard.edu/abs/2016AGUFMNG33D..01H/abstract>

268 Ilesanmi, B. O. and Moses, O. O. (2021). Estimation of Geoclimatic Factor for Nigeria  
269 through Meteorological Data, *European Journal of Electrical Engineering and*  
270 *Computer Science EJECE*. 5(3). ISSN: 2736-5751.  
271 <http://dx.doi.org/10.24018/ejece.2021.5.3.191>

272 ITU-R (2003). P.453-9, “The radio refractive index: its formula and refractivity data,”  
273 International Telecommunication Union, 2003.

274 ITU R (2012). P.453 - 11: The radio refractive index: its formula and refractivity data.  
275 [https://www.itu.int/dms\\_pubrec/itu-r/rec/p/R-REC-P.453-11-201507-S!!PDF-](https://www.itu.int/dms_pubrec/itu-r/rec/p/R-REC-P.453-11-201507-S!!PDF-E.pdf)  
276 [E.pdf](https://www.itu.int/dms_pubrec/itu-r/rec/p/R-REC-P.453-11-201507-S!!PDF-E.pdf)

277 ITU-R (09/2013). P.530-15. Propagation data and prediction methods required for the  
278 design of terrestrial line-of-sight systems

279 ITU-R P.530-14, 2012. Propagation data and prediction methods required for the design  
280 of terrestrial line-of-sight systems.

281 Karagianni, E. A., Mitropoulos, A.P., Latif, I.T., Kavousanos-Kavousanakis, A. G.,  
282 Koukos, J. A., & Fafalios M. E. (2014). Atmospheric Effects on EM  
283 Propagation and Weather Effects on the Performance of a Dual Band Antenna  
284 for WLAN Communications. NAUSIVIOS CHORA, 5.  
285 <https://nausivios.hna.gr/docs/2014B3.pdf>

286 Kolawole, L. B. (1983). Statistics of radio refractivity and atmospheric attenuation in  
287 tropical climates. *Proceedings of the URSI Commission F Symposium*, 69–75,  
288 Belgium.

289 Mason, S. P. (2010). Atmospheric effects on radio frequency (RF) wave propagation in  
290 a humid, near-surface environment. Theses and Dissertations. Naval  
291 Postgraduate School Monterey CA. Retrieved from  
292 <http://hdl.handle.net/10945/5353>.

293 Odedina, P. K. & Afullo, T. J. (2007), “Use of Spatial Interpolation Technique for the  
294 Determination of the Geoclimatic Factor and Fade Depth Calculation for  
295 Southern Africa,” Proceedings of IEEE AFRICON conference 2007 ISBN: 0 –  
296 7803 – 8606 – X. IEEE Catalogue number: 04CH37590C, September 26 – 28,  
297 2007, Namibia

298 Ononiwu, G. S. O. & Constance K. (2015). Determination of the Dominant Fading  
299 And The Effective Fading for The Rain Zones in the Itu-R P. 838-3  
300 Recommendation. *European Journal of Mathematics and Computer Science*.  
301 2(2), 17 -29. ISSN 2059-9951.

302 Ojo, O. L., Ajewole, M. O., Adediji, A. T., & Ojo, J. S. (2015). Estimation of Clear-Air  
303 Fades Depth Due to Radio Climatological Parameters for Microwave Link  
304 Applications in Akure, Nigeria. *International Journal of Engineering and  
305 Applied Sciences*. 7(3). ISSN2305-8269.

306 Řezáčová, D., Ondřej, F., & Lucas, R. (2003), Statistics of Radio Refractivity  
307 Derived from Prague Radio sounding Data, *Radio Engineering*. 12(4), 84-86

308 Shambayati, S. (2008). Atmosphere attenuation and noise temperature at microwave

309 frequencies. Low-Noise Systems in the Deep Space Network. Descanso  
310 9\_ch06\_020508.doc. 255-280.  
311 [https://descanso.jpl.nasa.gov/monograph/series10/06\\_Reid\\_chapt6.pdf](https://descanso.jpl.nasa.gov/monograph/series10/06_Reid_chapt6.pdf)

312 Tetzner, D., Thomas, E., & Allen, C. (2019). A validation of ERA5 reanalysis data  
313 in the Southern Antarctic Peninsula—Ellsworth land region, and its  
314 Implications for Ice Core Studies. *Geosciences*, 9(7), 289.  
315 doi:10.3390/geosciences9070289

316 Serdege, D., & Ivanovs, G. (2007). Refraction seasonal variation and influence onto  
317 GHZ range microwaves availability. *Electronics and Electrical Engineering*,  
318 78(6), 39-42.

319 Ugwu, E. B. I., Maureen, C. U., & Obiageli, J. U. (2015). Microwave propagation  
320 attenuation due to earth's atmosphere at very high frequency (VHF) and ultra-  
321 high frequency (UHF) bands in Nsukka under a clear air condition. *International*  
322 *Journal of Physical Sciences*, 10(11), 359-363. doi: 10.5897/IJPS2015.4358.

323 Valma, Z., Tamosiunaite, M., Tamosiunas S., Tamosiuniene, M., & Zilinskas, M.  
324 (2011). Variation of radio refractivity with height above ground. *Electronics and*  
325 *Electrical Engineering, Telecommunication Engineering*, 5, 23-26.

326 Zheng, S., & Han-Xian, F. (2013). Monitoring of ducting by using a ground-based gps  
327 receiver. *Chinese Physics B*, 22(2), 1-5.  
328 doi:10.1088/1674-1056/22/2/029301

329 Zubair, M., Haider, J. Y., Khan, S., & Nasir, J. (2011). Atmospheric influences on  
330 satellite communications. *Przegląd Elektrotechniczny*, 87(5), 261-264.  
331 <http://pe.org.pl/articles/2011/5/64.pdf>

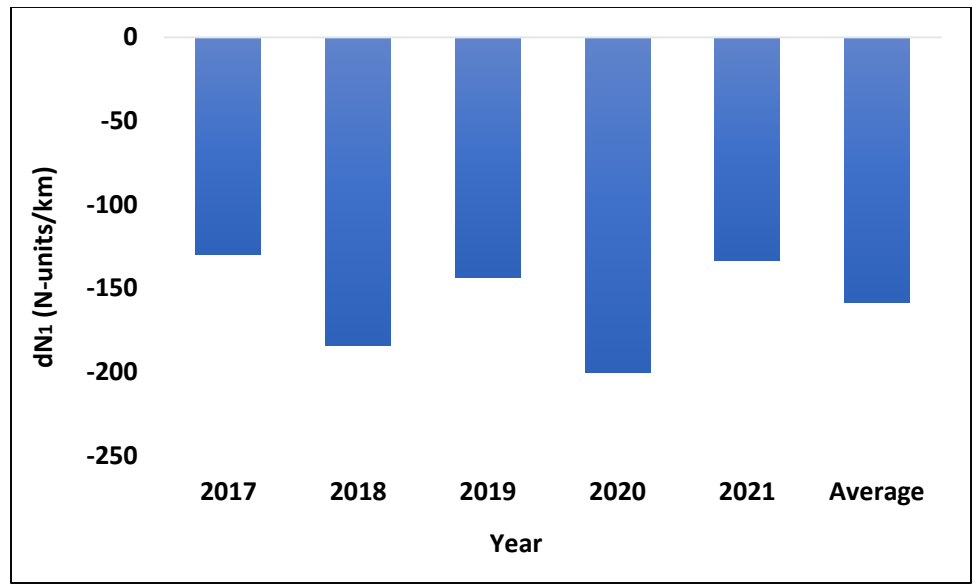


Figure 1: Yearly average of point refractivity gradient

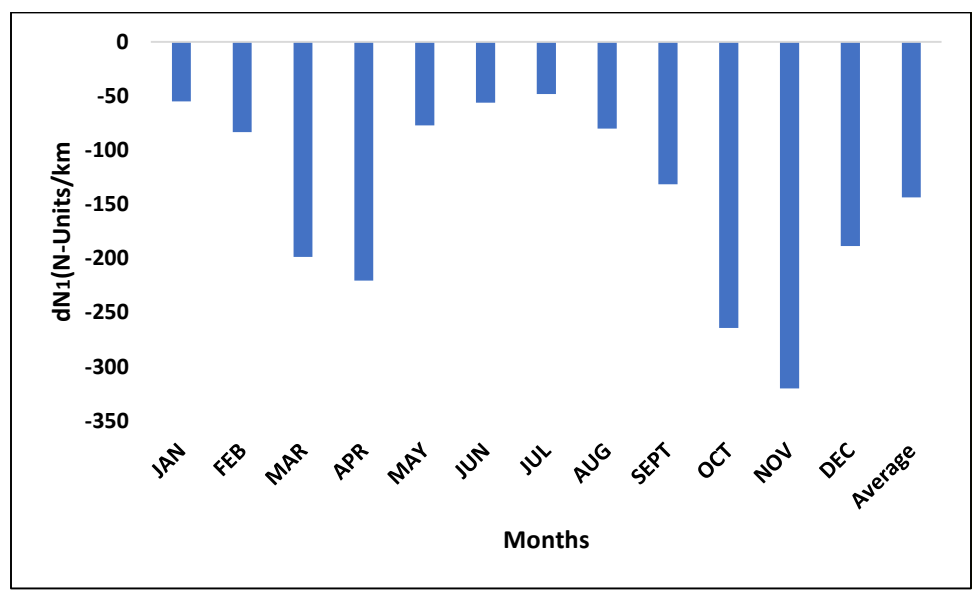
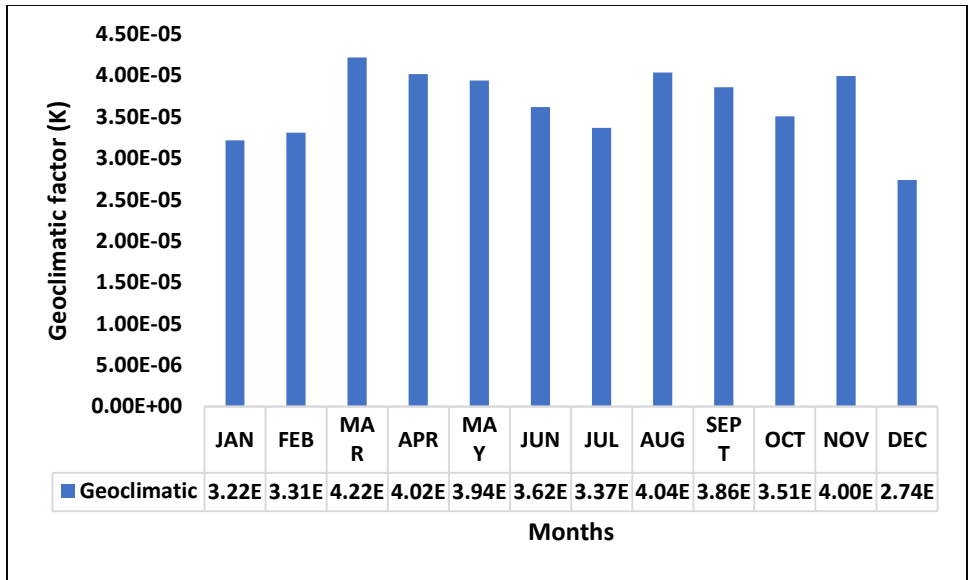
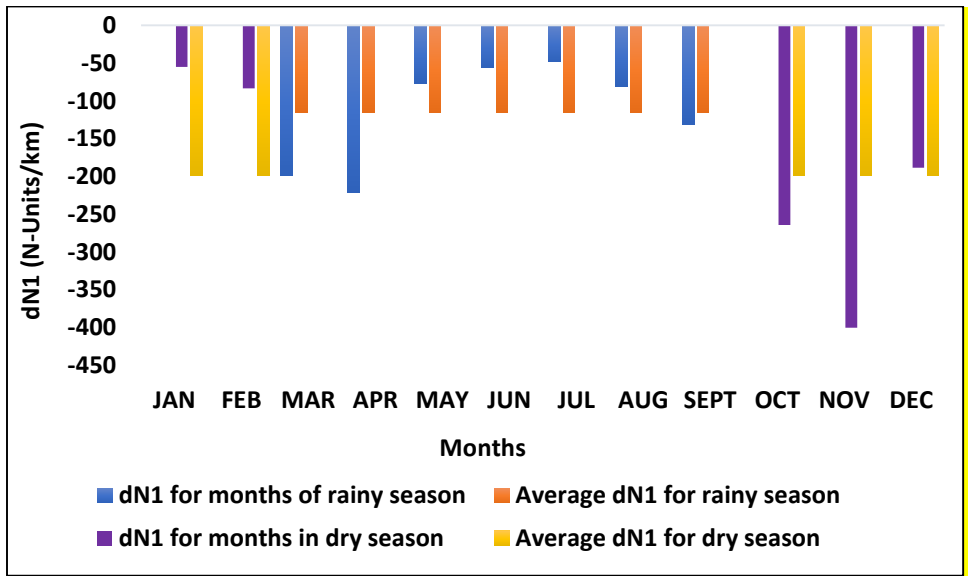


Figure 2: Monthly distribution of Point Refractivity Gradient (dN<sub>1</sub>)



**Figure 3: Monthly distribution of Geoclimatic Factor (K)**



**Figure 4: Point refractivity gradient for both dry and rainy months over Ede.**

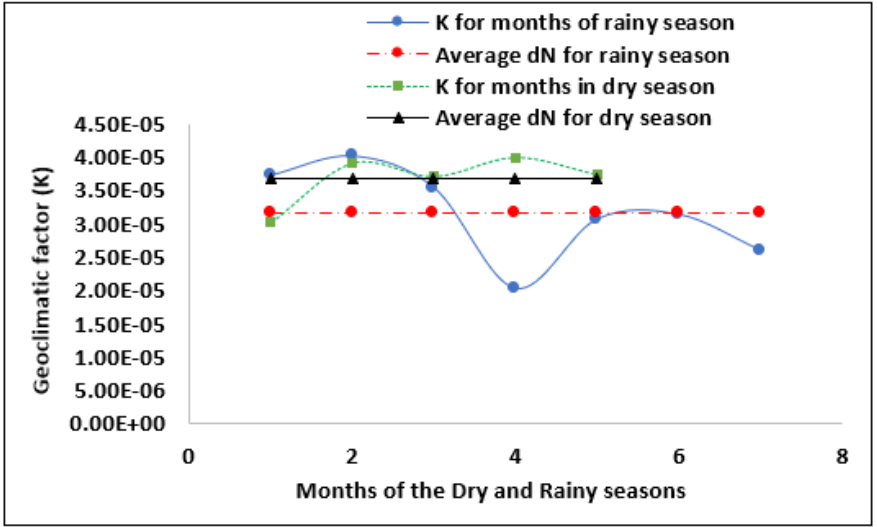


Figure 5: Dry and Rainy season monthly variation of Geoclimatic factor (K) over Ede

Table 1: Geoclimatic Factor (K) and Point Refractivity Gradient (dN<sub>1</sub>) for Ede on a monthly basis.

<b>MONTHS</b>	<b>GEOCLIMATIC FACTOR (K)</b>	<b>POINT REFRACTIVITY GRADIENT (dN<sub>1</sub> (N-units/Km))</b>
January	3.02E-05	-55.201
February	3.910E-05	-83.471
March	3.74E-05	-198.625
April	4.02E-05	-220-.713
May	3.54E-05	-77.254
June	2.02E-05	-56.311
July	3.07E-05	-48.332
August	3.14E-05	-80.142
September	2.60E-05	-131.631
October	3.71E-05	-180.510
November	4.00E-05	-225.542
December	3.74E-05	-320.144
Annual	3.37E-05	-143.712
Average		

Table 2: Monthly distribution of Point Refractivity Gradient (dN) for the dry and rainy seasons In Ede

Months of dry season	Point refractivity gradient of each month in the dry season	Months of rainy season	Point refractivity gradient of each month in the rainy season
Jan	-55.201	March	-198.625
Feb	-83.471	April	-220.713
Oct	-180.51	May	-77.254
Nov	-225.411	June	-56.311
Dec	-200.54	July	-48.332
		Aug	-80.142
Average point refractivity	-182.271	Sept	-131.631
		Average point refractivity	-116.17

Table 3: Monthly distribution of Geoclimatic factor (K) for the dry and rainy Season In Ede.

Months of dry season	Geoclimatic factor of each months in the dry season	Months of rainy season	Geoclimatic factor of each month in the rainy season
Jan	3.02E-05	March	3.74E-05
Feb	3.910E-05	April	4.02E-05
Oct	3.71E-05	May	3.54E-05
Nov	4.00E-05	June	2.02E-05
Dec	3.74E-05	July	3.07E-05
		Aug	3.14E-05
Average K for dry season	3.68E-05	Sept	2.60E-05
		Average K for rainy season	3.16E-05